Nanoscience and Nanotechnology Letters
Vol. 9, 1–8, 2017

Biostability Assessment of Silver Containing Hydroxyapatite Nanostructures

Sneha S. Bandgar[1,2], Tanaji V. Kolekar[3,4,*],

In the present study, Silver-modified hydroxyapatite (Ag–HA) (0, 0.5, 1.0, 1.5, 2.0, 2.5 mole%) nanoparticles were synthesized via simplistic combustion method using polyvinyl alcohol (PVA) as a fuel. Synthesized powder was studied by Thermo gravimetric analysis (TGA), X-ray diffraction (XRD), Scanning electron microscopy (SEM), Energy dispersive spectroscopy (EDS) and Transmission electron microscopy (TEM) with SAED techniques. The *in vitro* biocompatibility of silver substituted hydroxyapatite was studied. The biocompatibility of the Ag–HA nanoparticles was studied using L929 cell lines with MTT assays upto 24 h. MTT assay shows Ag-substituted HA nanoparticles have non-toxic interaction between L929 cell lines and the Ag-substituted HA, found to be biocompatible for further applications *in-vivo* systems. According to the obtained results, the synthesized nano composite powder confirms biocompatibility of Ag–HA and could be an attractive candidate for biomedical applications.

Keywords: Ag–Hydroxyapatite, MTT Assay, L929 Cells, Biomedical Applications.

1. INTRODUCTION

Scientists and engineers are actively engaged in developing nanocrystalline calcium orthophosphate (CaP) to enhance their biological and mechanical properties for their use in biomedical applications. CaP, have a large number of biomedical applications due to its biocompatibility.[1] In bone-tissue engineering, bioresorbable and bioactive phases of CaP bioceramic are preferred materials because of their similar composition natural bone, excellent osteoconductivity and biocompatibility.[2,3] The first report came in 1920, on the successful implication of CaP in human beings.[4] CaP are one of the most widely used bioresorbable and bioactive ceramics. If the Ca/P molar ratio is between 0.5 and 2.0 are known as non-ions substituted CaP and it gives organs stability and hardness of the tendons of mammals.[5] Among different forms of CaP, non-ions substituted hydroxyapatite (HA) is one of the most attractive bioinorganic materials. It is reported that Mineral constituents of HA and natural bones are same.[6]

Recently HA have been found applicable as a biocompatible material in surgery, bioengineering, and dentistry, because of its high bioresorbility and biocompatibility.[7] Synthetic HA's are having good positive ion (cation) exchange rate with some metals, excellent biocompatibility with high affinity for the pathogenic microorganisms.[8–10] In between 70–80% of artificial implants are made of biocompatible materials.[11] The incorporation of a transition metal ions like silver (Ag) in HA might be effective in controlling microorganisms due to its ion-exchange capabilities.[12] In bioengineering and biomedical applications have attracted synthetic HA doped with metal ions a lot due to its property like good flexibility and bio stability of CaP structure, a great number of cationic substitutions are of potential application in the bioengineering and biomedical field. Several reports available on the percentage of Ca sites by some divalent (Cd^{2+}, Sr^{2+}, Mg^{2+}, Ba^{2+}) and trivalent cations (Al^{3+}, Fe^{3+}).[13] Pazourková, et al. reported sorption of Cd^{2+} on hydroxyapatite nanostructure.[14] However, nowadays the biggest recent problem in the implanted synthetic biomaterials is

*Authors to whom correspondence should be addressed.

post-surgical infections because these biomaterials provide sites for potential bacterial adhesion.[15] When these biomaterials are exposed to aggressive body environment possible release of harmful metal ions takes place through wear and corrosion processes.[16–18] Continuous release of toxic metal ions causes adverse effects on the surrounding cells.[19–21] From many years, Ag has been known as a disinfectant and towards mammalian cells exhibiting low toxicity resulting in a broad spectrum of antimicrobial activity. Ag doped HA coatings are important in preventing bacterial adhesion.[22] If Ag used in nano-sized particles the reactivity of Ag is high due to their better contact with microorganisms.[23] The concentration of Ag more than 300 ppb in human blood can cause adverse effects in the form of leukopenia, liver damage etc. Therefore, the optimum concentration of Ag in HA is critical for efficient antimicrobial ability with less cytotoxicity.[24]

Nano-sized HA has been synthesized by various methods, like co-precipitation,[25] sol–gel techniques,[26] emulsion process,[27] microwave precipitation,[28] and mechanochemical methods.[29] Recently efforts have been reported toward the synthesis of biomaterials by solution combustion method.[30] Solution combustion technique has several advantages like varying ignition sources and the oxidizer/fuel ratio use of different oxidizers and fuels and controlling the synthesis parameters.[31]

In the present study, nanocrystalline Ag modified HA were prepared by a modified solution combustion method. Also, focuses on the result of Ag towards the biocompatibility of HA under the physical and biological conditions. The biocompatibility of nanocrystalline HA and Ag modified HA evaluated with different concentration by cytotoxicity assessments. Cytotoxicity of the synthesized nanomaterials has been evaluated with L929 (mouse fibroblast) cell line for 12 and 24 hr using MTT assays method.

2. EXPERIMENTAL DETAILS

2.1. Materials

Silver nitrate ($AgNO_3$) was purchased from Thomas Baker. Calcium nitrate tetrahydrate ($Ca(NO_3)_2 \cdot 4H_2O$), *di*-Ammonium hydrogen orthophosphate $(NH_4)_2HPO_4$ were purchased from Sigma-Aldrich. All chemicals used without any purification and all are analytical grade.

2.2. Synthesis of Ag-Doped Hydroxyapatite

Silver modified hydroxyapatite (Ag–HA) were prepared by a modified solution combustion with different concentration (0, 0.5, 1.0, 1.5, 2.0, 2.5 mole%).[32,33] Recently trans deposition method is reported for transition metal doped hydroxyapatite.[34] The stoichiometric amounts of the calcium precursors ($Ca(NO_3)_2 \cdot 4H_2O$), silver precursor ($AgNO_3$) and phosphate precursor ($(NH_4)_2HPO_4$) were dissolved in double distilled water molecule to get a final concentration of solution 0.1 M. Polyvinyl alcohol (PVA) was used as a fuel. In double distilled water molecule, the equimolar solution of PVA was prepared. The equimolar mixture of fuel and oxidants was stirred magnetically for 30 min at room temperature. After evaporation, this mixture form a gel of precursors at 100 °C and then this gel was heated at 300 °C to obtain a black coloured powder. The obtained powder of Ag–HA was then annealed at 950 °C for 6 h. The dried mixture can be ignited to start combustion reaction using muffle furnace. Various Ag–HA samples containing Ag content 0, 0.5, 1.0, 1.5, 2.0, 2.5 mole% were denoted as HA, Ag–HA-1, Ag–HA-2, Ag–HA-3, Ag–HA-4, Ag–HA-5 respectively.

2.3. Characterization

2.3.1. Structural and Morphological Studies

Crystal phase identification and structural analysis of Ag–HA were studied by X-ray diffraction (XRD) (Philip-3710) with Cu-Kα radiation. XRD patterns were analyzed by using software X-pert high score plus and obtained XRD patterns were then compared with standards established by the joint committee on powder diffraction and standards (JCDPS) to get correct phase structure matched with the standards card No. 01-074-0565 and 01-074-1743). Thermo gravimetric analysis (TGA) is a used for thermal analysis in which changes in chemical and physical properties of materials are measured with a constant heating rate as a function of increasing temperature. Particle size and morphology was observed by using by using transmission electron microscope (TEM, JEOLJEM-2100) with the resolution of 2.4 Å. The elemental analysis was done by energy dispersive spectroscopy (EDS, JEOL JSM 6360).

2.4. Biocompatibility Study

2.4.1. Cell Culture

Cytotoxicity of Ag–HA samples was carried out on L929 (mouse fibroblast) out by using MTT assay. The L929 cell lines were obtained from national center for cell sciences, Pune (India). *In vitro* cytotoxicity was carried out at national toxicology center, (NTC) pune (ISO 10993/USP 32 NF 27). The L929 (mouse fibroblast) cells were cultured in dulbecco's modified Eagle medium containing 10% fetal bovine serum, (0.1 mg/mL), sodium bicarbonate (1.5 $mg \cdot mL^{-1}$) and penicillin G (100 U/mL) at 37 °C in an atmosphere containing 5% CO_2. *In vitro* cytotoxicity of Ag–HA was carried out in MTT assays.

2.4.2. MTT Assay

It has been reported elsewhere that, MTT assay to test *in vitro* cytotoxicity of different nanomaterials.[35] The L929 cells (2×10^5 cells $\cdot mL^{-1}$) were incubated for 24 h in a 96-well microtiter plate in the respective medium. After complete completion 24 h, the old media was replaced by fresh media and different concentration of sterile Ag–HA (0.0, 0.2, 0.4, 0.6, 0.8 and 1 mg/mL of culture media).

Then the total medium was incubated in a 5% CO_2 atmosphere at 37 °C for 12 and 24 h. Then after 12 and 24 h, 10 μl of 5 mg/ml MTT solution was added to each well including control wells and the plates were incubated for 3 h in a 5% CO_2 atmosphere at 37 °C for metabolization of MTT assay with the Ag–HA nanoparticles and cell media. In the cell wells only anchored cells remained when the total old medium was removed by flicking the plates. Then the cells were washed with PBS (phosphate buffer saline) and the formazan formed was extracted in 200 μl acidic isopropanol in each well and after 1 hr, absorbance was recorded at 570 nm from which cell viability was calculated. The experiments were repeated three times and the mean data were taken for the graph. The relative cell viability (%) compared with control well-containing cells without nanoparticles are calculated by the equation:

$$\text{Relative cell viability (\%)} = [A_{\text{absorbance}}]_{\text{tested}}/[A_{\text{absorbance}}]_{\text{control}} \times 100 \quad (1)$$

3. RESULTS AND DISCUSSION

3.1. Thermogravimetric Analysis

TGA curve of pure HA and Ag–HA-5 are shown in Figure 1. Total five different stages were observed during the total weight loss. In between room temperature to 250 °C the first stage was observed due to weight loss because of loss of physically adsorbed water molecules.[36, 37] Due to loss of organic groups, chemisorbed water molecules and attached solvent to the sample the second stage of weight loss is occurs at 250 to 450 °C. The third stage is from 450 to 650 °C, the fourth stage is from 650 to 870 °C and the last fifth stage is from 870 °C. In the fifth stage the weight loss is less than 0.65%. Consideration of TGA studies, all the samples of Ag–HA are calcinated at 950 °C for further characterization and studies.

3.2. XRD Analysis

The XRD patterns of pure HA and Ag–HA samples were shown in Figure 2. Compared with pure HA, no new peaks were detected for Ag–HA samples even the doping concentration increased (0.0, 0.5, 1.0, 1.5, 2.0, 2.5 mole%). The XRD characteristic peaks of hydroxyapatite for each sample could be assigned to standard one (JPCDS no. 00-024-0033). No diffraction peaks of elemental silver or silver phosphate were detectable. This revels that the silver dose not exist as a separate phase with sufficient crystallinity. However, the crystallinity of HA changes with increasing Ag content due to the formation of silver phosphate (JCPDS no. 01-084-0192). HA showing space group $P6_3/m$ with a hexagonal structure. Primary peak (222), (210), (211) and (220) confirm that synthesized material is HA and secondary peak (202) and (113) are confirming the presence of small amount of Ag in HA. Scherrer equation was used to calculate crystallite size (D) from the gaussian fit of the most intense peak (211).

$$D = \frac{0.9\lambda}{\beta \cos\theta} \quad (2)$$

Where, λ is the wavelength of Cu-Kα radiations (λ = 1.5405 Å), β is full width at half maxima of the most intense peak (211), θ is the corresponding Braggs diffraction angle and D is the crystallite size. The average crystallite sizes of HA and Ag–HA were found to be 28.50 nm and 22.12 nm, respectively. The reflection peaks are quite broad, suggesting their nano crystalline and pure nature. XRD of Ag–HA shows similar peaks with previously reported work.[38]

3.3. SEM Analysis

Figure 3 depicted SEM micrographs of Ag–HA powder are shown agglomerates that are consisting of small size and fine crystallites. It has been reported that in bone

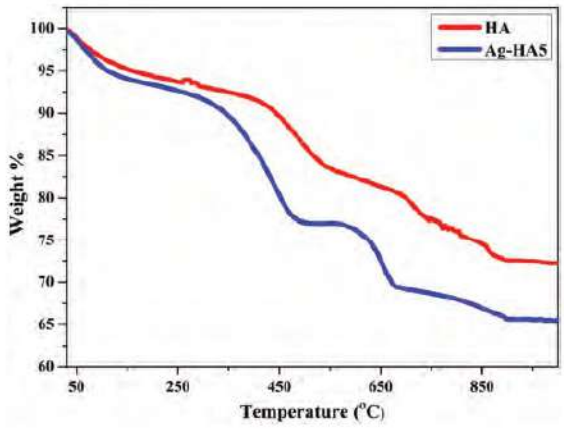

Fig. 1. TGA pattern of pure HA and Ag–HA-5 nanoparticles.

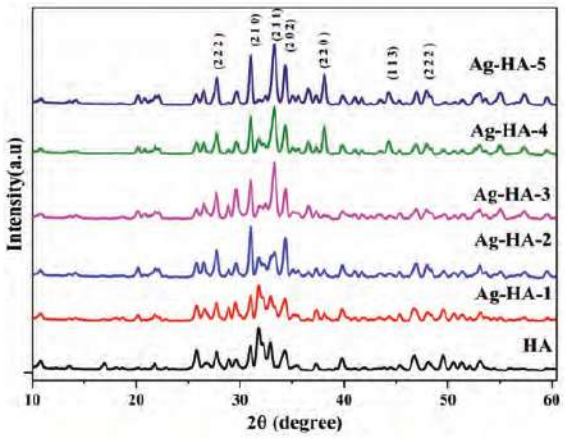

Fig. 2. XRD patterns of pure HA and Ag–HA nanoparticles.

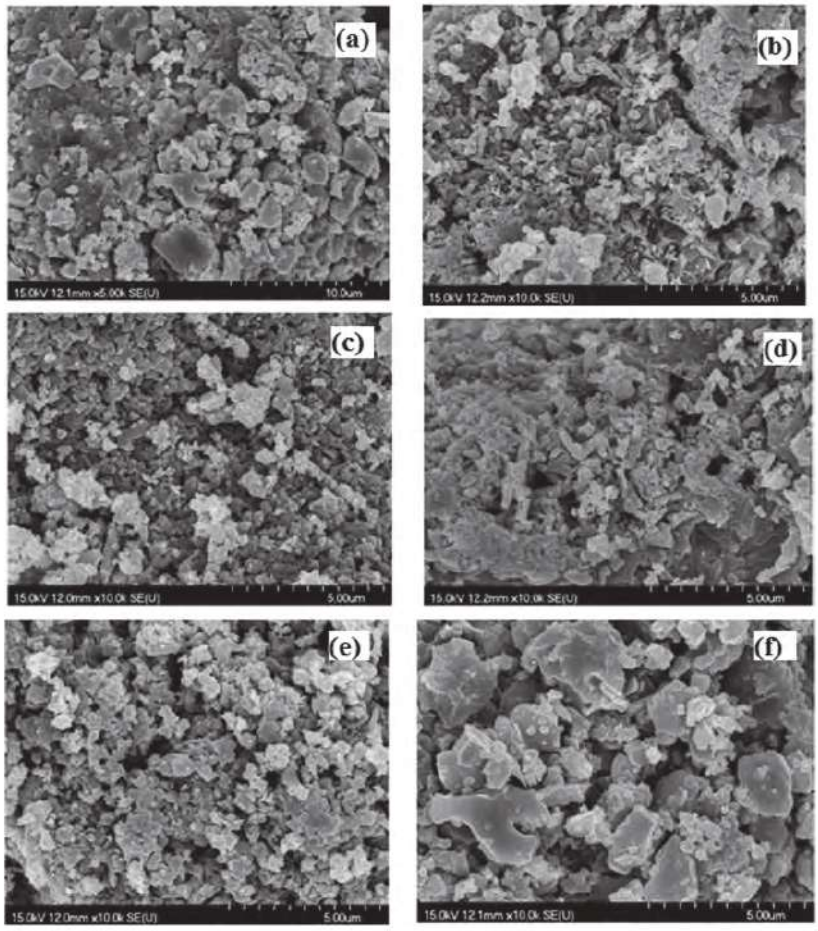

Fig. 3. SEM images of (a) pure HA, (b) Ag–HA-1, (c) Ag–HA-2, (d) Ag–HA-3, (e) Ag–HA-4, and (f) Ag–HA-5.

fracture crystal size distribution of bone material plays an important role.[39] To estimate the elemental composition of Ag–HA samples EDS analysis were carried out. EDS spectra of all Ag–HA samples are shown in Figure 4. The EDS spectra show expected stoichiometry and elemental signals indicate that samples are consistent and pure. The peaks correspond to silver (Ag), calcium (Ca), phosphor (P), and oxygen (O) were observed in Ag–HA samples while the peaks correspond to oxygen (O), calcium (Ca) and phosphor (P) were detected for pure HA sample. The elemental composition of Ag–HA from EDS analysis is in Table I. The standard Ca/P atomic ratio is 1.67, from EDS analysis. The Ca/P atomic ratios for pure nanocrystalline HA is 1.66 which is near to standard. The Ca/P atomic ratios (1.51, 1.48, 1.46, 1.45, 1.42) for Ag–HA samples are near to that of the standard. It has been observed. There is a slightly decrease in Ca/P atomic ratio in the Ag–HA samples (Table I). Table II shows atomic ratio and particle size of HA and Ag–HA sample. From the table, it is clear that as the percentage of Calcium decreases it decreases the particle size. The obtained results reveal that proper substitution of Ca with Ag metal ion during the synthesis process. It has been reported that Ca/P atomic ratios between 1.33–1.55 could be very beneficial to the formation of new bone *in vivo*.[40] Thus, Ag–HA could be good candidature for the formation of new bone *in vivo*. Obtained atomic ratios suggest that samples are stoichiometric.

3.4. TEM Studies

TEM images of HA and Ag–HA-5 are shown in Figure 5. It observed that, pure HA nanoparticles were a rod-like shape and around 100 nm in diameter with homogeneous microstructure, most particles seem to be good aggregates. Hence particle sizes of Ag–HA-5 about 100 nm and decreased significantly with the existence of Ag element. Crystal sizes obtained from XRD are slightly smaller than observed crystal sizes it's because of high-temperature calcination (950 °C) which cause the grain size growth and due to the presence of nanocrystalline surface layers.

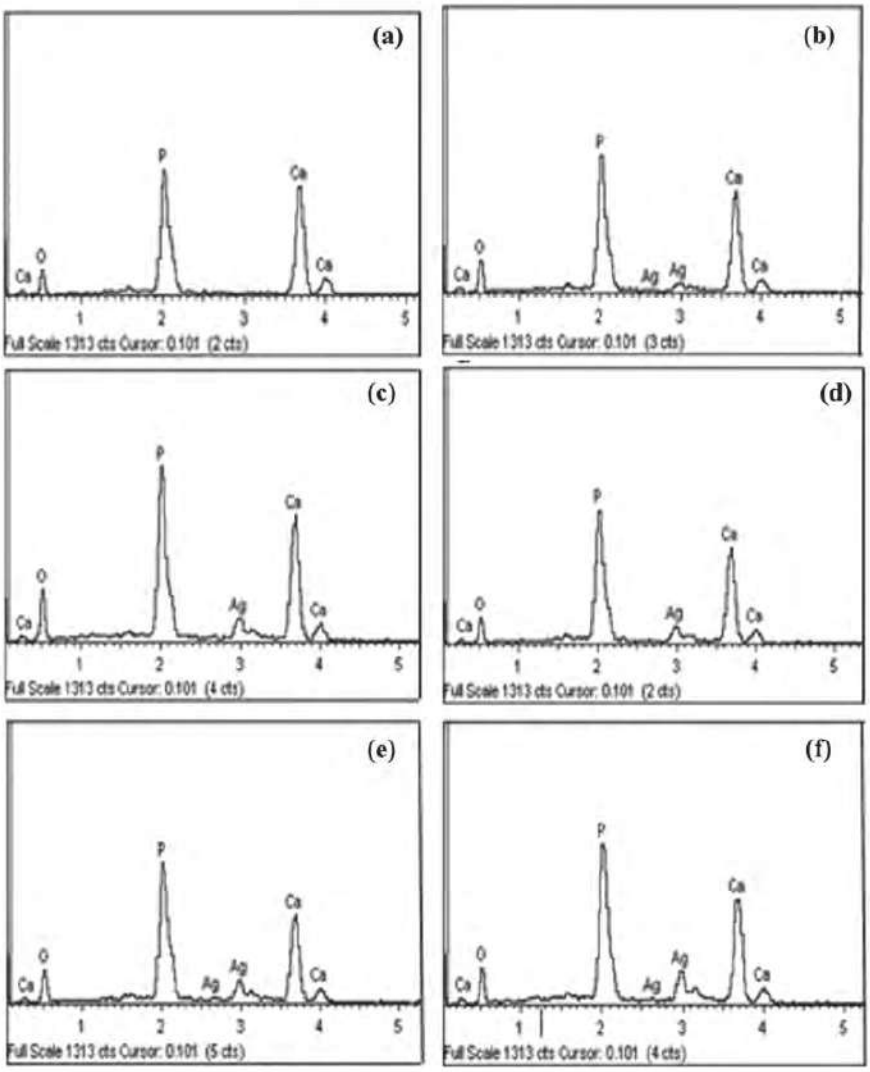

Fig. 4. EDS spectrum of (a) pure HA, (b) Ag–HA-1, (c) Ag–HA-2, (d) Ag–HA-3, (e) Ag–HA-4, and (f) Ag–HA-5.

Figures 5(a) and (b) shows SAED patterns of HA and Ag–HA-5 shows in the inset of. The presence of bright ring patterns confirms polycrystalline nature of Ag–HA nanoparticles.

Table I. Elemental composition of HA and Ag–HA nanoparticles.

	Atomic % composition			
Sample	Ag	Ca	P	O
HA	–	32.33	19.52	48.15
Ag–HA-1	1.02	28.89	19.03	51.06
Ag–HA-2	1.51	28.13	18.97	51.40
Ag–HA-3	3.27	26.97	18.40	57.68
Ag–HA-4	4.48	23.12	15.93	58.29
Ag–HA-5	6.07	21.90	15.33	60.21

3.5. Cytotoxicity Study

The effect of different concentrations and incubation time of Ag–HA nanoparticles on the cell viability was evaluated against L929 cell lines. It is reported that if the Dextran-Capped Silver Nanoparticles evaluated by the changes

Table II. Atomic ratio and particle size of HA and Ag–HA nanoparticles.

Sr.no.	Name of sample	Atomic ratio (Ca/P)	Particle size (nm)
1	HA	1.66	28.50
2	Ag–HA-1	1.51	22.85
3	Ag–HA-2	1.48	22.28
4	Ag–HA-3	1.46	22.34
5	Ag–HA-4	1.45	22.07
6	Ag–HA-5	1.42	21.06

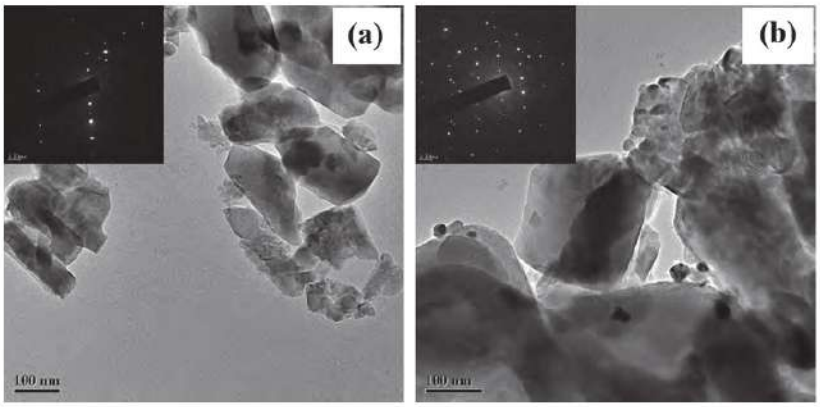

Fig. 5. TEM images of (a) HA, (b) Ag–HA-5 (Inset: Corresponding SAED pattern).

of cell morphology and 3-(4,5-dimethylthiazol-2-yl)-2,5-diphenyl-tetrazolium bromide assay. Results shows that these silver nanoparticles had slight effect on the survival and proliferation of L-929 cells.[41] Figures 6(a)–(d) shows the obtained data. *In vivo* L929 cell lines were interact with HA, Ag–HA-1, Ag–HA-3, Ag–HA-5 nanoparticles for 12 h and 24 h, respectively with the concentration of 0.2, 0.4, 0.6, 0.8, and 1 $mg \cdot mL^{-1}$ in a 5% CO_2 atmosphere at 37 °C. Shi et al. reported that, optical density values directly proportional to relative cell viability with respect

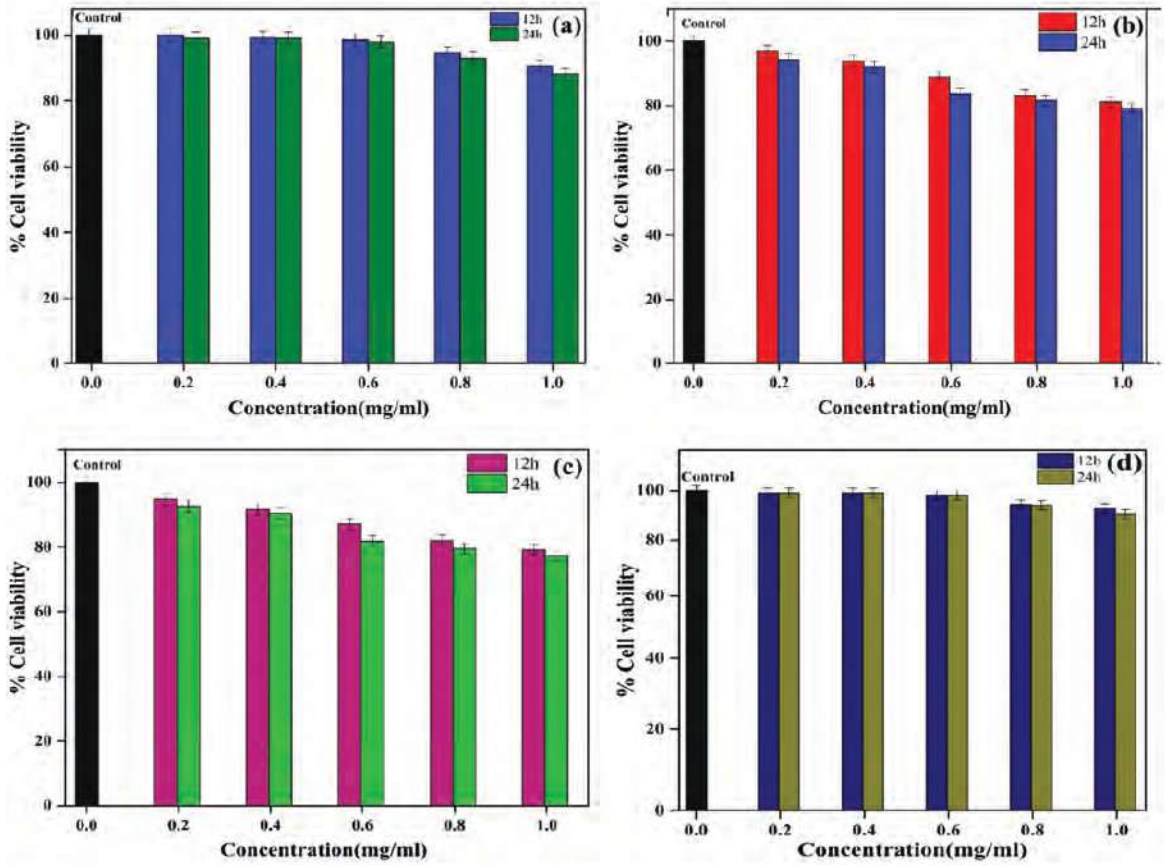

Fig. 6. Cytotoxicity profiles of (a) pure HA, (b) Ag–HA-1, (c) Ag–HA-3, (d) Ag–HA-5 for 12 and 24 hr.

to the concentration of nanoparticles (50–1000 μg/mL) and very low cell viability of nanoparticles on cells for the cell cytotoxicity HA and Ag–HA against L929 cell lines for 12 h and 24 h.[42] As compared to positive control it shows that low extract concentration of Ag–HA have less cytotoxicity and higher extract concentration accelerate slight toxic effect to L929 cells.

As increasing concentration and incubation time of Ag–HA nanoparticles, the cell viability gradually decreases of all four Ag–HA samples. Decreasing the grain sizes increasing cell cytotoxicity. The cellular inflammatory reaction is generally enhanced by plasma membrane invagination when the particle size is in the range of 100 nm.[43] In comparison with the previous reports, the result obtained for our samples shows that the Ag–HA having very low cytotoxicity towards L929 cell lines. It has been observed that, no major difference in the cytotoxicity of HA and Ag–HA nanoparticles. This is accredited to a relatively small change composition (Ca/P ratio) with the difference in the particle size. The obtained results from cytotoxicity experiments reveals better biocompatibility of HA and Ag–HA nanoparticles with a concentration up to 1 mg $\cdot$ mL^{-1}. The cytotoxicity study on L929 cells of HA and Ag–HA nanoparticles synthesized by modified solution combustion technique, here confirmed that the biological effects are not only based on chemical composition but also on size, shape, and surface texture and aggregation state.

4. CONCLUSIONS

Modified solution combustion technique has been employed to facile synthesize HA nanoparticles in which Ca is partially substituted by Ag. Addition of Ag precursor under a controlled condition which leads to Ag–HA with a Ca/P ratio very similar to standard one. The structural, morphological, compositional, cytotoxicity and antimicrobial properties of the HA and Ag–HA nanoparticles with different stoichiometric ratios have been studied in great detail. The physical and chemical properties of the HA have been modified by the presence of Ag. The HA and Ag–HA nanoparticles having no any secondary phase and almost identical particle sizes. EDS analysis confirmed the presence of HA and Ag–HA with the Ca/P ratio similar to the standard ratio and this material could be applicable to the formation of new bone *in vivo*. The results of this work demonstrate the applicability of Ag–HA nanoparticles in the biomedical field. Furthermore, the cytotoxicity studies show that the Ag–HA lower cytotoxicity. Hence, it is proved that Ag–HA nanocrystals are potentially applicable as bone substitution materials in biomedical application. Ag–HA is an excellent material in the tissue engineering. The ultra-trace Ag-doped HA nanocrystals may provide new opportunities for a non-cytotoxic implant with antimicrobial ability in tissue engineering.

References and Notes

1. A. Bigi, E. Boanini, and K. Rubini, *J. Solid State Chem.* 177, 3092 **(2004)**.
2. L. L. Hench, *Bioceramics J. American Ceramic Society* 81, 1705 **(1998)**.
3. K. D. Groot, C. P. A. T. Klein, J. G. C. Wolke, and J. M. A. Blieck-Hogervorst, Calcium phosphate and hydroxyapatite ceramics, Handbook of Bioactive Ceramics, edited by T. Yamamuro, L. L. Hench, and J. Wilson, CRC Press, Boca Raton, FL **(1990)**, Vol. 2, p. 3.
4. R. Z. LeGeros, *International Symposium on New Wave of Ceramics for the 21st Century at the 40th Symposium on Basic Science of Ceramics, Convention Center*, Osaka University **(2002)**.
5. Monika Supovan, *Ceram. Int.* 41, 9203 **(2015)**.
6. H. J. Qiu, J. Yang, P. Kodali, J. Koh, and G. A. Ameer, *Biomaterials* 27, 5845 **(2006)**.
7. Y. Tanaka, Y. Hirata, and R. Yoshinaka, *J. Ceram. Process. Res.* 4, 197 **(2003)**.
8. I. Smiciklas, A. Onjia, J. Markovic, and S. Raicevic, *Mater. Sci. Forum* 494, 405 **(2005)**.
9. R. Z. LeGeros, *Chem. Rev.* 108, 4742 **(2008)**.
10. E. D. Berry and G. R. Siragusa, *Appl. Environ. Microbial.* 63, 4069 **(1997)**.
11. M. Niinomi, M. Nakai, and J. Hieda, *Acta Biomaterialia* 8, 3888 **(2012)**.
12. K. S. Oh, K. J. Kim, Y. K. Jeong, and Y. H. Choa, *Key Eng. Mater.* 240–242, 583 **(2003)**.
13. M. Wakamura, K. Kandori, and T. Ishikawa, *Colloids Surface: A* 164, 297 **(2000)**.
14. L. Pazourková, J. Kupková, H. Marianna, S. Jana, and M. G. Simha, *J. Nanosci. Nanotechnol.* 16, 7788 **(2016)**.
15. E. M. Hetrick and M. H. Schoenfisch, *Chem. Soc. Rev.* 35, 780 **(2006)**.
16. U. Türkan, O. Öztürk, and A. E. Eroğlu, *Surface and Coatings Technology* 200, 5020 **(2006)**.
17. N. Espallargas, C. Torres, and A. I. Muñoz.
18. S.-J. Lee and J.-J. Lai, *Journal of Materials Processing Technology* 140, 206 **(2003)**.
19. C.-C. Shih, C.-M. Shih, Y.-Y. Su, L. H. J. Su, M.-S. Chang, and S.-J. Lin, *Corrosion Science* 46, 427 **(2004)**.
20. T. F. Zhang, Q. Y. Deng, B. Liu, B. J. Wu, F. J. Jing, Y. X. Leng, et al., *Surface and Coatings Technology*.
21. B. Alemón, M. Flores, W. Ramírez, J. C. Huegel, and E. Broitman, *Tribology International* 81, 159 **(2015)**.
22. V. Stanic, D. Janackovic, S. Dimitrijevic, S. B. Tanaskovic, M. Mitrica, M. S. Pavlovic, A. Krstic, D. Jovanovic, and S. Raicevic, *Appl. Surf. Sci* 257, 4510 **(2011)**.
23. J. R. Morones, J. L. Elechiguerra, A. Camacho, K. Holt, J. B. Kouri, J. T. Ramirez, and M. J. Yacaman, *Nanotechnology* 16, 2346 **(2005)**.
24. C. Shi, J. Gao, M. Wang, J. Fu, D. Wang, and Y. Zhu, *Mater. Sci. Eng. C* 55, 497 **(2015)**.
25. R. Murugan and S. Ramakrishna, *Acta Biomater.* 2, 201 **(2006)**.
26. M. H. Fathi, A. Hanifi, and V. Mortazavi, *J. Mater. Process. Technol.* 202, 536 **(2008)**.
27. G. C. Koumoulidis, A. P. Katsoulidis, A. K. Ladavos, P. J. Pomonis, C. C. Trapalis, A. T. Sdoukos, and T. C. Vaimakis, *J. Colloid Interface Sci.* 259, 254 **(2003)**.
28. Z. Zou, K. Lin, L. Chen, and J. Chang, *Ultrason. Sonochem.* 19, 1174 **(2012)**.
29. S. Lala, S. Brahmachari, P. K. Das, D. Das, T. Kar, and S. K. Pradhan, *Mater. Sci. Eng. C* 42, 647 **(2014)**.
30. A. G. Merzhanov, 40 Years of SHS: A Lucky Star of Scientific Discovery, Bentham Science **(2012)**, e-book, Vol. 112.
31. S. T. Aruna, Solution combustion synthesis—An overview, Combustion Synthesis: Novel Routes to Novel Materials, edited by M. Lackner, Bentham Publishers **(2010)**, pp. 206–221.

32. Tanaji V. Kolekar, Nanasaheb D. Thorat, Hemraj M. Yadav, Veeresh T. Magalad, Mahesh A. Shinde, Sneha S. Bandgar, Jin H. Kim, and Ganesh L. Agawane, *Ceramic International* 42, 5304 (**2016**).

33. Sneha S. Bandgar, Hemraj M. Yadav, Shailesh S. Shirguppikar, Mahesh A. Shinde, Rajendra V. Shejawal, Tanaji V. Kolekar, and Sambhaji R. Bamane, *Journal of the Korean Ceramic Society* 54, 158 (**2017**).

34. H. Setsiri, P. Thinnaphat, N. Medena, E. Somsook, Y. Yakiyama, Raghu Nath Dhital, and H. Sakurai, *J. Nanosci. Nanotechnol.* 17, 4649 (**2017**).

35. N. D. Thorat, S. V. Otari, R. M. Patil, V. M. Khot, A. I. Prasad, R. S. Ningthoujam, et al., *Colloids Surf. B Biointerfaces* 111, 264 (**2013**).

36. A. J. Nathanael, D. Mangalaraj, P. C. Chen, and N. Ponpandian, *J. Nanopart. Res.* 13, 1841 (**2011**).

37. I. S. Kim and P. N. Kumta, *Mater. Sci. Eng. B* 111, 232 (**2004**).

38. F. A. C. Andradea, L. C. O. Vercikb, F. J. Monteiroc, and E. C. S. Rigoa, *Ceram. Int.* 42, 2271 (**2016**).

39. M. J. Phillips, J. A. Darr, Z. B. Luklinska, and I. Rehman, *J. Mater. Sci. Mater. Med.* 14, 875 (**2003**).

40. S. V. Dorozhkin, *Prog. Cryst. Growth Charact. Mater.* 44, 45 (**2002**).

41. G. Yang, Q. Lin, C. Wang, J. Li, J. Wang, J. Zhou, Y. Wang, and C. Wang, *J. Nanosci. Nanotechnol.* 12, 3766 (**2012**).

42. C. Shi, J. Gao, M. Wang, J. Fu, D. Wang, and Y. Zhu, *Material Science and Engineering C* 55, 497 (**2015**).

43. A. E. Nel, L. Mädler, D. Velegol, T. Xia, E. M. V. Hoek, P. Somasundaran, et al., *Nat. Mater.* 8, 543 (**2009**).

Received: 21 February 2017. Accepted: 31 May 2017.